

Locally Non-centrosymmetric Superconductivity in Multilayer Systems

Daisuke MARUYAMA*, Manfred SIGRIST¹, and Youichi YANASE²

Graduate School of Science and Technology, Niigata University, Niigata 950-2181, Japan

¹Theoretische Physik, ETH-Honggerberg, 8093 Zurich, Switzerland

²Department of Physics, Niigata University, Niigata 950-2181, Japan

Although multilayer systems possess *global* inversion symmetry, some of the layers lack *local* inversion symmetry because no global inversion centers are present on such layers. Such locally non-centrosymmetric systems exhibit spatially modulated Rashba spin-orbit coupling. In this study, the superconductivity in multilayer models exhibiting inhomogeneous Rashba spin-orbit coupling is investigated. We study the electronic structure, superconducting gap, and spin susceptibility in the superconducting state with mixed parity order parameters. We show the enhancement of the spin susceptibility by Rashba spin-orbit coupling and interpret it on the basis of the crossover from a centrosymmetric superconductor to a non-centrosymmetric superconductor. It is also shown that the spin susceptibility is determined by the phase difference of the order parameter between layers and is nearly independent of the parity mixing of order parameters. An intuitive understanding is given on the basis of the analytic expression of superconducting order parameters in the band basis. The results indicate that not only a broken *global* inversion symmetry but also a broken *local* inversion symmetry leads to unique properties of superconductivity. We discuss the superconductivity in artificial superlattices involving CeCoIn₅ and multilayer high- T_c cuprates.

KEYWORDS: superconductivity without local inversion symmetry, spin susceptibility, multilayer system

1. Introduction

The discovery of superconductivity in the heavy-fermion compound without inversion symmetry, CePt₃Si,¹⁾ triggered extensive studies of non-centrosymmetric superconductivity.²⁾ Subsequently, several new non-centrosymmetric superconductors with unique properties have been identified among heavy-fermion materials and in other classes of materials.^{3–17)} The research field has even been effectively extended to non-centrosymmetric superfluids in cold Fermi gases^{18,19)} in which antisymmetric spin-orbit coupling is artificially induced. Many interesting properties, such as the parity mixing of order parameters,²⁰⁾ the magnetoelectric effect,^{21–24)} anisotropic spin susceptibility,^{20,25–32)} accompanied by an anomalous paramagnetic depairing effect,³³⁾ helical superconducting phases in a magnetic field,^{33–39)} and topological superfluid phases,¹⁸⁾ have been proposed and studied in various contexts.

The term non-centrosymmetric superconductivity is commonly used for systems that have no inversion center. It is, however, interesting to note that features familiar in non-centrosymmetric superconductors can also be relevant for systems with an inversion center, but specific forms of a local violation of inversion symmetry. A clear example is a multilayer system in which the local mirror symmetry is broken, as shown in Fig. 1. Naturally, the question arises whether superconductivity displays any exotic property in such a *locally* non-centrosymmetric system. One of the authors has earlier investigated this issue by studying the spin triplet superconducting state with random Rashba spin-orbit coupling arising from stacking faults.⁴⁰⁾ In this study, we focus on regular multilayer systems and elucidate the

basic properties of such *locally* non-centrosymmetric superconductors. We show that, indeed, some properties of the superconducting phase can be strongly affected by a broken local inversion symmetry in multilayer systems that exhibit small interlayer coupling.



Fig. 1. (Color online) Schematic view of trilayer system with focus on local inversion symmetry. The inversion center is present in the inner layer; it is absent in the outer layers. This crystal structure is regarded as a locally non-centrosymmetric system.

Our study is motivated by the observation of superconductivity in artificial superlattices consisting of the heavy-fermion superconductor CeCoIn₅ and the conventional metal YbCoIn₅.^{41,42)} Although it is expected that the superconductivity occurs in sufficiently thick multilayer structures of CeCoIn₅, it is surprising that it even prevails down to superlattice incorporating stacks of only three well-separated CeCoIn₅ layers.

The superconductivity in bulk CeCoIn₅ has attracted considerable interest for its unique magnetic features, such as the paramagnetic depairing effect,⁴³⁾ the possible realization of the Fulde-Ferrell-Larkin-Ovchinnikov phase at high magnetic fields,^{44,45)} an unconventional magnetic order,^{46,47)} and field-induced quantum criticality.^{48–52)} These features make it even more attractive to investigate the superconductivity in superlattices of

CeCoIn₅. As such, it represents an ideal system for studying the effects of *local* inversion symmetry breaking, and more so because many of the striking properties of non-centrosymmetric superconductors may result from the additional presence of strong magnetic correlations.

A better class of systems of similar character is that of multilayer high- T_c cuprates.^{53–55} Although cuprate superconductors have been intensively investigated since their discovery in 1986, the role of spatially modulated Rashba spin-orbit coupling has not received much attention thus far. Since the magnetic properties of multilayer cuprates are investigated by nuclear magnetic resonance (NMR) measurement, it is also possible to study multilayer cuprates focusing on local non-centrosymmetry. For instance, the spin susceptibility in the superconducting state can be measured with a layer resolution using the Knight shift of NMR. Following a brief report on the spin susceptibility in locally non-centrosymmetric systems,⁵⁶ we study here the electronic structure, superconducting gap, and spin susceptibility of multilayer superconductors in detail.

The paper is organized as follows. In §2, we introduce the model Hamiltonian for multilayer systems including spatially modulated Rashba spin-orbit coupling and parity-mixed superconducting order parameters. In §3, we show the numerical results of the spin susceptibility in the bi- and tri-layer systems to demonstrate the crossover from a conventional superconductor to a non-centrosymmetric superconductor. The numerical results are discussed on the basis of analytic expressions for the electronic structure (§4) and superconducting gap (§5) by decomposing the spin susceptibility into the Pauli and Van-Vleck parts (§6). The relationship between the symmetry of order parameters and the spin susceptibility is clarified in §7, where a nontrivial role of the interlayer phase difference of order parameters is discussed. The numerical results of the spin susceptibility in more than three layers are shown in §8. A brief summary and discussion of the superconductivity in CeCoIn₅ are given in §9.

2. Model

First, we introduce a model Hamiltonian for two-dimensional multilayer superconductors with spatially modulated Rashba spin-orbit coupling as

$$H = H_b + H_{\text{SOC}} + H_{\text{pair}} + H_{\perp}, \quad (1)$$

$$H_b = \sum_{\mathbf{k}, s, m} \varepsilon(\mathbf{k}) c_{\mathbf{k}sm}^{\dagger} c_{\mathbf{k}sm}, \quad (2)$$

$$H_{\text{SOC}} = \sum_{\mathbf{k}, s, s', m} \alpha_m \mathbf{g}(\mathbf{k}) \cdot \boldsymbol{\sigma}_{ss'} c_{\mathbf{k}sm}^{\dagger} c_{\mathbf{k}s'm}, \quad (3)$$

$$H_{\text{pair}} = \frac{1}{2} \sum_{\mathbf{k}, s, s', m} [\Delta_{ss'm}(\mathbf{k}) c_{\mathbf{k}sm}^{\dagger} c_{-\mathbf{k}s'm}^{\dagger} + \text{h.c.}], \quad (4)$$

$$H_{\perp} = t_{\perp} \sum_{\mathbf{k}, s, \langle m, m' \rangle} c_{\mathbf{k}sm}^{\dagger} c_{\mathbf{k}s'm'}, \quad (5)$$

where $c_{\mathbf{k}sm}$ ($c_{\mathbf{k}sm}^{\dagger}$) is the annihilation (creation) operator for an electron with spin s on layer m , and $\boldsymbol{\sigma}_{ss'}$ is the Pauli matrix of the Pauli matrices.

The first term, H_b , describes the dispersion relation without spin-orbit coupling or interlayer coupling. We consider a square lattice and assume a tight-binding model, i.e., $\varepsilon(\mathbf{k}) = -2t(\cos k_x + \cos k_y) - \mu$. The (x, y, z) -axes correspond to the (a, b, c) -axes of the tetragonal crystal structure. We choose the unit of energy as $t = 1$ and fix the chemical potential $\mu = -1$, which leads to the electron density per site being approximately 0.63. The following results are nearly independent of the dispersion relation and electron density.

The second term, H_{SOC} , describes the Rashba spin-orbit coupling arising from the lack of local inversion symmetry. This term preserves time reversal symmetry, if the \mathbf{g} -vector is odd in \mathbf{k} , i.e., $\mathbf{g}(-\mathbf{k}) = -\mathbf{g}(\mathbf{k})$. The coupling constants α_m should have opposite signs between layers above and below the inversion center so as to conserve global inversion symmetry. For instance, $(\alpha_1, \alpha_2, \alpha_3) = (\alpha, 0, -\alpha)$ for trilayers. For $\mathbf{g}(\mathbf{k})$, the multilayer systems should have a Rashba-type \mathbf{g} -vector because the mirror symmetry is broken for outer layers (see Fig. 1). Although the detailed momentum dependence of $\mathbf{g}(\mathbf{k})$ is determined by electronic structures,³² we assume here the simple form $\mathbf{g}(\mathbf{k}) = (-\sin k_y, \sin k_x, 0)$.

The third term, H_{pair} , introduces intralayer Cooper pairing via an off-diagonal mean field. We ignore interlayer pairing as we consider the layers to be weakly coupled. Since we take into account the spatially modulated Rashba spin-orbit coupling arising from a broken local inversion symmetry, the order parameter $\Delta_{ss'm}(\mathbf{k})$ involves both spin singlet and triplet components,

$$\Delta_{ss'm}(\mathbf{k}) = \begin{pmatrix} -d_{xm}(\mathbf{k}) + id_{ym}(\mathbf{k}) & \psi_m(\mathbf{k}) + d_{zm}(\mathbf{k}) \\ -\psi_m(\mathbf{k}) + d_{zm}(\mathbf{k}) & d_{xm}(\mathbf{k}) + id_{ym}(\mathbf{k}) \end{pmatrix}, \quad (6)$$

where $\psi_m(\mathbf{k})$ and $\mathbf{d}_m(\mathbf{k})$ are the corresponding scalar and vector order parameters for the spin singlet and triplet pairings on the layer m , respectively. For our discussion, we avoid the use of a microscopic model based on a pairing mechanism. Rather, we introduce an order parameter on phenomenological grounds, which we assume to have s -wave symmetry for the singlet pairing and a p -wave symmetry for the triplet pairing. On symmetry grounds, we choose $\psi_m(\mathbf{k}) = \psi_m$ and $\mathbf{d}_m(\mathbf{k}) = d_m \mathbf{g}(\mathbf{k}) = d_m(-\sin k_y, \sin k_x, 0)$. We take $|\psi_m|, |d_m| \leq 0.01$ to be sufficiently small to satisfy the condition $|\Delta_{ss'm}(\mathbf{k})| \ll |\alpha_m| \ll \varepsilon_F$ (ε_F is the Fermi energy), as realized in most non-centrosymmetric superconductors. To minimize the interlayer coupling energy, the dominant order parameter component maintains the same sign over all layers, whereas the other (subdominant) component adjusts the sign to that of spin-orbit coupling (α_m).

The fourth term, H_{\perp} , describes the interlayer hopping of electrons between nearest-neighbor layers. Since we consider a quasi-two-dimensional system, we assume that the interlayer hopping t_{\perp} is smaller than the intralayer hopping t .

3. Numerical Results of Spin Susceptibility

3.1 Spin susceptibility for fields along c -axis

We now determine the spin susceptibility of multilayer superconductors for spatially modulated Rashba spin-orbit coupling, with a magnetic field applied along the c -axis. The spin susceptibility $\chi = \lim_{H \rightarrow 0} \langle M_s \rangle / H$ is obtained by calculating the magnetization $\langle M_s \rangle$ in the field \mathbf{H} . The Zeeman coupling term is introduced as

$$H_Z = -\frac{g\mu_B}{2} \sum_{\mathbf{k}, s, s', m} \mathbf{H} \cdot \boldsymbol{\sigma}_{ss'} c_{\mathbf{k}sm}^\dagger c_{\mathbf{k}s'm}, \quad (7)$$

where we assume $g = 2$ and μ_B is the Bohr magneton. First, the Hamiltonian is diagonalized by introducing the unitary transformation $\hat{C}_{\mathbf{k}}^\dagger = \hat{\Gamma}_{\mathbf{k}}^\dagger \hat{U}^\dagger(\mathbf{k})$ in the Nambu space of M layers, where quasi-particle operators form a $4M$ -dimensional vector,

$$\hat{C}_{\mathbf{k}}^\dagger = (c_{\mathbf{k}\uparrow 1}^\dagger, c_{\mathbf{k}\downarrow 1}^\dagger, c_{-\mathbf{k}\uparrow 1}, c_{-\mathbf{k}\downarrow 1}, \dots, \dots, c_{\mathbf{k}\uparrow M}^\dagger, c_{\mathbf{k}\downarrow M}^\dagger, c_{-\mathbf{k}\uparrow M}, c_{-\mathbf{k}\downarrow M}), \quad (8)$$

and are analogous to the Bogoliubov quasi-particle operators $\hat{\Gamma}_{\mathbf{k}}^\dagger = (\gamma_{\mathbf{k}1}^\dagger, \gamma_{\mathbf{k}2}^\dagger, \dots, \gamma_{\mathbf{k}4M}^\dagger)$. The diagonalized Hamiltonian is written as

$$H + H_Z = \frac{1}{2} \sum_{\mathbf{k}} \sum_{i=1}^{4M} E_i(\mathbf{k}) \gamma_{\mathbf{k}i}^\dagger \gamma_{\mathbf{k}i}, \quad (9)$$

where $E_i(\mathbf{k})$ is the quasi-particle energy. The magnetization is given as

$$\langle M_s \rangle = \frac{g\mu_B}{2} \sum_{\mathbf{k}} \sum_{i=1}^{4M} [\hat{S}^z(\mathbf{k})]_{ii} f(E_i(\mathbf{k})), \quad (10)$$

where $f(E)$ is the Fermi-Dirac distribution function. The matrix representation of a spin operator is defined on the $\hat{\Gamma}_{\mathbf{k}}^\dagger$ basis as

$$\hat{S}^\mu(\mathbf{k}) = \hat{U}^\dagger(\mathbf{k}) \hat{\Sigma}^\mu \hat{U}(\mathbf{k}), \quad (11)$$

with $\hat{\Sigma}^\mu$ as the μ -component of the spin operator in the $4M$ -dimensional space.

We now focus on the spin susceptibility of bilayer ($M = 2$) and trilayer ($M = 3$) systems at zero temperature. More than three layers will be discussed in §8. The corresponding coupling constants of Rashba spin-orbit coupling are described as $(\alpha_1, \alpha_2) = (\alpha, -\alpha)$ for bilayers and $(\alpha_1, \alpha_2, \alpha_3) = (\alpha, 0, -\alpha)$ for trilayers.

We compare two cases: (A) the spin triplet channel is dominant $|d| > |\psi|$ and (B) the spin singlet channel is dominant $|\psi| > |d|$. The order parameters are assumed as follows:

- (A) $(\psi_1, \psi_2) = (\psi, -\psi)$ and $(d_1, d_2) = (d, d)$ for bilayers.
 $(\psi_1, \psi_2, \psi_3) = (\psi, 0, -\psi)$ and $(d_1, d_2, d_3) = (d, d, d)$ for trilayers.
- (B) $(\psi_1, \psi_2) = (\psi, \psi)$ and $(d_1, d_2) = (d, -d)$ for bilayers.
 $(\psi_1, \psi_2, \psi_3) = (\psi, \psi, \psi)$ and $(d_1, d_2, d_3) = (d, 0, -d)$ for trilayers.

In case (A), the spin susceptibility remains unaffected by the superconductivity $\chi_s = \chi_n$ because the spin triplet component of the type $\mathbf{d}_m(\mathbf{k}) \propto \mathbf{g}(\mathbf{k}) \perp \hat{z}$ is an equal-spin pairing state with Cooper pair spins along the c -axis. The spin susceptibility is independent of the interlayer coupling

possible without pair breaking. This feature is essentially independent of spin-orbit coupling, interlayer hopping, and the number of layers, as can be seen in Figs. 2 and 3 for both bi- and tri-layer systems, respectively. We will provide more rigorous arguments for this kind of behavior in §7.

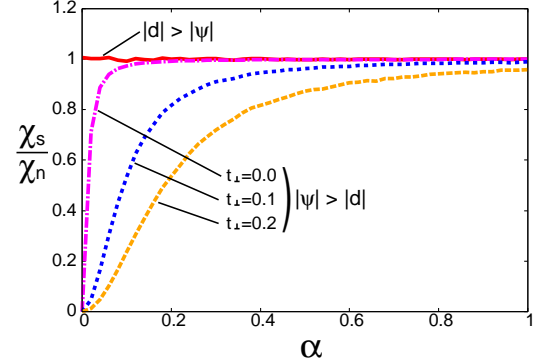


Fig. 2. (Color online) Spin susceptibility along c -axis for bilayer system. The interlayer coupling t_\perp is shown in the figure for the dominantly spin singlet pairing state (dashed, dotted, and dash-dotted lines). The spin susceptibility is independent of interlayer coupling when the spin triplet channel is dominant (solid line). We assume that $\psi = 0.01$ and $d = 0$ in the former, and $\psi = 0$ and $d = 0.01$ in the latter. The spin susceptibility is nearly independent of the subdominant order parameter, as will be shown in Fig. 5.

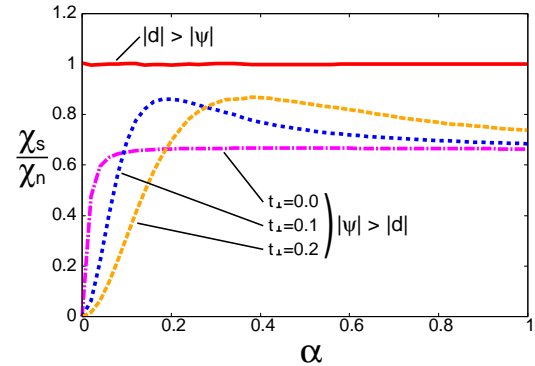


Fig. 3. (Color online) Spin susceptibility along c -axis for trilayer system. The interlayer coupling t_\perp is shown in the figure for the dominantly spin singlet pairing state (dashed, dotted, and dash-dotted lines). The spin susceptibility is independent of interlayer coupling when the spin triplet channel is dominant (solid line). The spin susceptibility is nearly independent of the subdominant order parameter as in the bilayer system (Fig. 5).

More interesting is case (B), as spin singlet pairing leads to a complete suppression of the spin susceptibility at $T = 0$ in a conventional superconductor. Indeed for a vanishing spin-orbit coupling ($\alpha = 0$), we find $\chi_s = 0$ irrespective of t_\perp . As soon as spin-orbit coupling is turned on, however, the spin susceptibility gradually recovers and approaches a constant value for large α : $\chi_s \rightarrow \chi_n$ for the bilayer and $\chi_s \rightarrow 2\chi_n/3$ for the trilayer. The mechanism of this behavior is different from the one in case (A), where the spin susceptibility is independent of the interlayer coupling.

by Rashba-type spin-orbit coupling (see §4). Note that the layers behave as being nearly decoupled for large α , and then the spin susceptibility along c -axis is recovered for layers with non-vanishing α_m . Consequently, in the bilayer system, all layers are involved, giving rise to a full recovery of χ_s for large α (analogous to the uniformly non-centrosymmetric superconductor²⁸), whereas in the trilayer system, only two of the three layers can contribute to what yielding a correspondingly reduced limiting value of $\chi_s = 2\chi_n/3$. Figure 4 corroborates this picture by considering the contributions of the different layers. Indeed, in a large- α regime, the outer layers $m = 1, 3$ carrying spin-orbit coupling saturate at $\chi_s \rightarrow \chi_n/3$, while the center layer $m = 2$ completely suppresses the spin susceptibility. Remarkably, at small α ($< t_\perp$), χ_s behaves in the same way for all layers and surprisingly leads to a nonmonotonic α -dependence for the center layer.

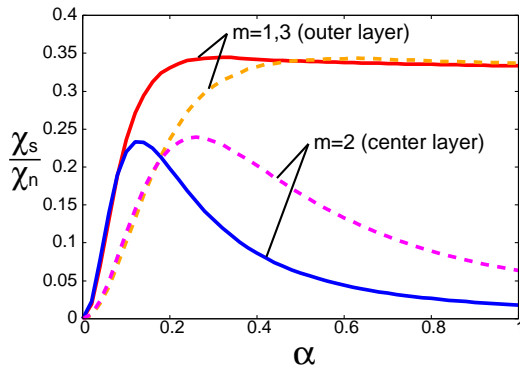


Fig. 4. (Color online) Contribution of each layer to spin susceptibility along c -axis in trilayer system. We assume the spin singlet state ($\psi = 0.01$ and $d = 0$) with $t_\perp = 0.1$ (solid line) and $t_\perp = 0.2$ (dashed line).

The numerical data in Figs. 2 and 3 show that interlayer hopping is in competition with spatially modulated Rashba spin-orbit coupling, such that a larger t_\perp yields a higher effective $\alpha_{\text{eff}} \sim t_\perp$ for the crossover from the behavior of a conventional superconductor to that of a non-centrosymmetric superconductor. For $\alpha_{\text{eff}} \gg t_\perp$, layers are almost decoupled from each other (see §4), and then the multilayer superconductor is regarded as a set of (non-)centrosymmetric superconductors. This crossover is best observed in the peak of χ_s at approximately $\alpha_{\text{eff}} \sim t_\perp$ for the center layer of the trilayer system (Fig. 4). Thus, modifying t_\perp , e.g., by applying uniaxial stress along the c -axis, can affect the magnetic response for c -axis fields in case (B). No such effect is expected in case (A).

Surprisingly, these results are almost independent of the subdominant order parameter. Figure 5 shows the spin susceptibility of bilayers for various $|\psi|$ values while keeping the summation $|\psi| + |d| = 0.01$. We see a nearly constant spin susceptibility except for the jump at $|\psi| = |d| = 0.005$. This jump arises from a discontinuous change of the order parameter, since we assume case (A) for $|\psi| < |d|$ and case (B) for $|\psi| > |d|$. We will show that this jump is similar to that of the spin susceptibility

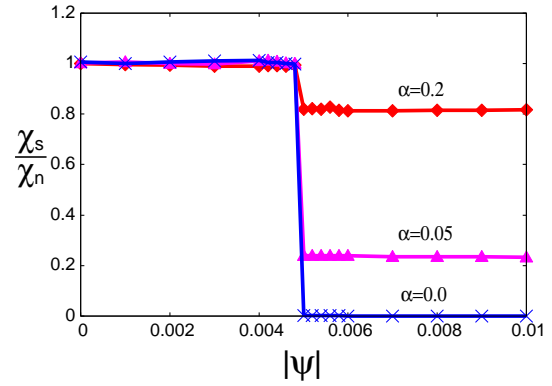


Fig. 5. (Color online) Zero-temperature spin susceptibility along c -axis for various $|\psi|$ values in bilayer system. We assume the amplitude of the spin triplet component to be $|d| = 0.01 - |\psi|$. We show the results for interlayer coupling $t_\perp = 0.1$ and spin-orbit coupling $\alpha = 0$ (crosses), $\alpha = 0.05$ (triangles), and $\alpha = 0.2$ (diamonds).

the interlayer phase differences of order parameters (§7). Since we assume the zero-phase difference for the dominant order parameter and the π -phase difference for the subdominant one, the spin susceptibility is determined by the dominant order parameter and is negligibly affected by the subdominant component. The details will be given in §7.

3.2 Spin susceptibility along ab -axis

Within our model, we find that the spin susceptibility along the ab -axis is always half of that along the c -axis, independent of the strength of α and t_\perp as well as of the number of layers. For numerical evidence, Fig. 6 shows the spin susceptibility along the ab -axis in the trilayer system; it is one-half of the results in Fig. 3. We confirmed these behaviors for another number of layers.

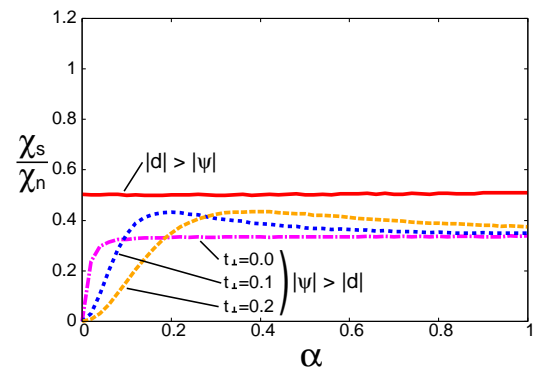


Fig. 6. (Color online) Spin susceptibility along a -axis for trilayer system. Parameters are the same as those in Fig. 3.

4. Electronic Structure in Normal State

To elucidate the crossover from the behavior of a centrosymmetric superconductor to that of a non-centrosymmetric superconductor shown in the numerical calculation (Figs. 2 and 3), we give an analytic expression of the band structure of the normal state. The band structure

gap in §4 and §5, respectively. An intuitive understanding is given in §6 by decomposing the spin susceptibility into the Pauli and Van-Vleck parts.

4.1 Bilayer system

First, we study the single-particle wave function in the normal state of bilayer systems. The schematic figure for the role of Rashba spin-orbit coupling and interlayer coupling is shown in Fig. 7. When the two layers are decoupled at $t_{\perp} = 0$, each layer has Fermi surfaces, as shown in Fig. 7. The structures of Fermi surfaces are the same for layers 1 and 2, but the spin orientations are opposite, because the Rashba spin-orbit coupling α_m has the opposite sign $\alpha_1 = -\alpha_2$. When the interlayer coupling t_{\perp} is switched on, the Fermi surfaces are coupled, as shown by dashed arrows in Fig. 7.

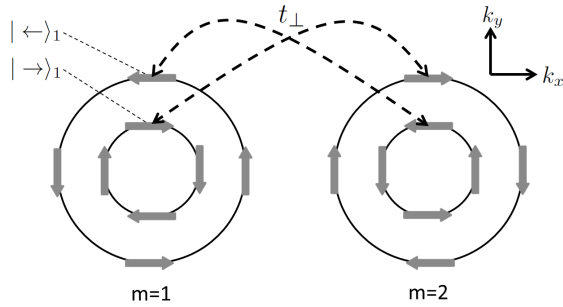


Fig. 7. Schematic figure of Fermi surfaces in bilayer system without interlayer coupling $t_{\perp} = 0$. In this case, layers are decoupled, and then the Fermi surfaces of layers 1 and 2 are independent of each other. The Fermi surfaces are split by Rashba spin-orbit coupling in both layers 1 and 2, but the spin orientations are opposite because Rashba spin-orbit coupling α_m has the opposite sign ($\alpha_1 = -\alpha_2$). When interlayer coupling t_{\perp} is tuned on, the electronic states are coupled, as shown by dashed arrows.

We show the wave function of quasi-particles with the momentum $\mathbf{k} = (0, k_y)$ as an example. According to the Fermi surfaces shown in Fig. 7, a simple expression is obtained by choosing the spin quantization axis along the x -direction. In the following presentation, the wave functions $|\rightarrow\rangle_m$ and $|\leftarrow\rangle_m$ describe the electron states on the layer m with right- and left-pointing spins, respectively. In the normal state with $\Delta_{ss'm}(\mathbf{k}) = 0$, the Hamiltonian [eq. (1)] is block-diagonalized in this representation. The block of the Hamiltonian is obtained as

$$\begin{pmatrix} \varepsilon(\mathbf{k}) + \alpha'(\mathbf{k}) & t_{\perp} \\ t_{\perp} & \varepsilon(\mathbf{k}) - \alpha'(\mathbf{k}) \end{pmatrix} \text{ for } \begin{pmatrix} |\rightarrow\rangle_1 \\ |\rightarrow\rangle_2 \end{pmatrix}, \quad (12)$$

and

$$\begin{pmatrix} \varepsilon(\mathbf{k}) - \alpha'(\mathbf{k}) & t_{\perp} \\ t_{\perp} & \varepsilon(\mathbf{k}) + \alpha'(\mathbf{k}) \end{pmatrix} \text{ for } \begin{pmatrix} |\leftarrow\rangle_1 \\ |\leftarrow\rangle_2 \end{pmatrix}, \quad (13)$$

respectively. We denote the magnitude of spin-orbit coupling as

$$\alpha'(\mathbf{k}) \equiv \alpha |\mathbf{g}(\mathbf{k})| = \alpha \sqrt{\sin^2 k_x + \sin^2 k_y}. \quad (14)$$

Diagonalizing the 2×2 matrix, we obtain eigenvalues

with twofold degeneracy:

$$E_1^{(2)}(\mathbf{k}) = \varepsilon(\mathbf{k}) + \sqrt{\alpha'(\mathbf{k})^2 + t_{\perp}^2}, \quad (15)$$

$$E_2^{(2)}(\mathbf{k}) = \varepsilon(\mathbf{k}) - \sqrt{\alpha'(\mathbf{k})^2 + t_{\perp}^2}. \quad (16)$$

The wave function is obtained as

$$\begin{cases} \sqrt{1 - A(\mathbf{k})^2} |\rightarrow\rangle_1 + A(\mathbf{k}) |\rightarrow\rangle_2 \\ A(\mathbf{k}) |\leftarrow\rangle_1 + \sqrt{1 - A(\mathbf{k})^2} |\leftarrow\rangle_2 \end{cases}, \quad (17)$$

for $E = E_1^{(2)}(\mathbf{k})$ and as

$$\begin{cases} -A(\mathbf{k}) |\rightarrow\rangle_1 + \sqrt{1 - A(\mathbf{k})^2} |\rightarrow\rangle_2 \\ \sqrt{1 - A(\mathbf{k})^2} |\leftarrow\rangle_1 - A(\mathbf{k}) |\leftarrow\rangle_2 \end{cases}, \quad (18)$$

for $E = E_2^{(2)}(\mathbf{k})$. We here defined

$$A(\mathbf{k}) \equiv \frac{t_{\perp}}{\sqrt{t_{\perp}^2 + (\alpha'(\mathbf{k}) + \sqrt{\alpha'(\mathbf{k})^2 + t_{\perp}^2})^2}}. \quad (19)$$

We obtain a similar single-particle wave function for the other momentum $k_x \neq 0$ by choosing a spin quantization axis parallel to $\mathbf{g}(\mathbf{k})$.

The twofold degeneracy in the above two energy bands originates from the time-reversal and global inversion symmetry. Thus, the structure of the energy bands seems to be the same as that in conventional metals. However, Rashba spin-orbit coupling affects the single-particle wave function in a unique way. Note that $A(\mathbf{k})$ in eq. (19) is determined by the competition between interlayer coupling t_{\perp} and spin-orbit coupling α . When spin-orbit coupling is absent, i.e., $\alpha = 0$, eq. (19) is reduced to $A(\mathbf{k}) = 1/\sqrt{2}$. Then, two energy bands are regarded as bonding and antibonding bands with spin degeneracy, namely, $(1/\sqrt{2})(|\rightarrow\rangle_1 + |\rightarrow\rangle_2)$ and $(1/\sqrt{2})(|\leftarrow\rangle_1 + |\leftarrow\rangle_2)$ for $E = E_1^{(2)}(\mathbf{k})$, and $(1/\sqrt{2})(|\rightarrow\rangle_1 - |\rightarrow\rangle_2)$ and $(1/\sqrt{2})(|\leftarrow\rangle_1 - |\leftarrow\rangle_2)$ for $E = E_2^{(2)}(\mathbf{k})$, respectively. This is the conventional band structure of bilayer systems. On the other hand, we obtain $A(\mathbf{k}) = 0$ in the limit of large spin-orbit coupling $\alpha \gg t_{\perp}$, and then the twofold degeneracy is given by $|\rightarrow\rangle_1$ and $|\leftarrow\rangle_2$, and by $|\leftarrow\rangle_1$ and $|\rightarrow\rangle_2$. Thus, the quasi-particle is localized on each layer and degenerates with a quasi-particle of opposite spin on the other layer. In this case, the splitting of the two energy bands is induced by the spin splitting in each layer, although the twofold degeneracy is protected by the global inversion symmetry. With increasing spin-orbit coupling, the two energy bands change their character from the bonding and antibonding states to the spin split states on each layer. This crossover leads to the α dependence of spin susceptibility in Fig. 2.

4.2 Trilayer system

Next, we study the trilayer systems. The single-particle wave function is obtained in the same way as that in the bilayer system. Figure 8 shows the schematic figure of Fermi surfaces in the decoupling limit $t_{\perp} = 0$. For the quasi-particles with $\mathbf{k} = (0, k_y)$, the Hamiltonian without

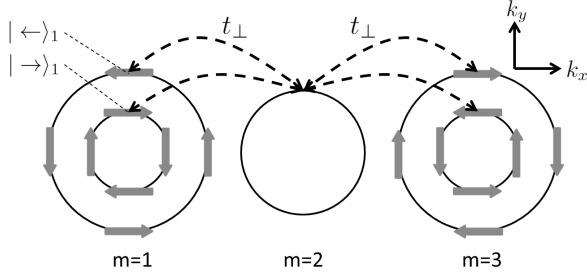


Fig. 8. Schematic figure of Fermi surfaces in trilayer system without interlayer coupling $t_{\perp} = 0$. Fermi surfaces in layers 1 and 3 are split by Rashba spin-orbit coupling; however, they degenerate in layer 2 because of $\alpha_2 = 0$. When interlayer coupling t_{\perp} is turned on, the electronic states are coupled, as shown by dashed arrows.

pairing field $\Delta_{ss'm}(\mathbf{k}) = 0$ is block-diagonalized as

$$\begin{pmatrix} \varepsilon(\mathbf{k}) + \alpha'(\mathbf{k}) & t_{\perp} & 0 \\ t_{\perp} & \varepsilon(\mathbf{k}) & t_{\perp} \\ 0 & t_{\perp} & \varepsilon(\mathbf{k}) - \alpha'(\mathbf{k}) \end{pmatrix} \text{ for } \begin{pmatrix} |\rightarrow\rangle_1 \\ |\rightarrow\rangle_2 \\ |\rightarrow\rangle_3 \end{pmatrix}, \quad (20)$$

and as

$$\begin{pmatrix} \varepsilon(\mathbf{k}) - \alpha'(\mathbf{k}) & t_{\perp} & 0 \\ t_{\perp} & \varepsilon(\mathbf{k}) & t_{\perp} \\ 0 & t_{\perp} & \varepsilon(\mathbf{k}) + \alpha'(\mathbf{k}) \end{pmatrix} \text{ for } \begin{pmatrix} |\leftarrow\rangle_1 \\ |\leftarrow\rangle_2 \\ |\leftarrow\rangle_3 \end{pmatrix}. \quad (21)$$

Diagonalizing the 3×3 matrix, we obtain three eigenvalues:

$$E_1^{(3)}(\mathbf{k}) = \varepsilon(\mathbf{k}) + \sqrt{\alpha'(\mathbf{k})^2 + 2t_{\perp}^2}, \quad (22)$$

$$E_2^{(3)}(\mathbf{k}) = \varepsilon(\mathbf{k}), \quad (23)$$

$$E_3^{(3)}(\mathbf{k}) = \varepsilon(\mathbf{k}) - \sqrt{\alpha'(\mathbf{k})^2 + 2t_{\perp}^2}, \quad (24)$$

with twofold degeneracy. The wave function is described as

$$\begin{cases} \sqrt{1 - B^2 - C^2} |\rightarrow\rangle_1 + C |\rightarrow\rangle_2 + B |\rightarrow\rangle_3 \\ B |\leftarrow\rangle_1 + C |\leftarrow\rangle_2 + \sqrt{1 - B^2 - C^2} |\leftarrow\rangle_3 \end{cases}, \quad (25)$$

for $E = E_1^{(3)}(\mathbf{k})$,

$$\begin{cases} -C |\rightarrow\rangle_1 + \sqrt{1 - 2C^2} |\rightarrow\rangle_2 + C |\rightarrow\rangle_3 \\ C |\leftarrow\rangle_1 + \sqrt{1 - 2C^2} |\leftarrow\rangle_2 - C |\leftarrow\rangle_3 \end{cases}, \quad (26)$$

for $E = E_2^{(3)}(\mathbf{k})$, and

$$\begin{cases} B |\rightarrow\rangle_1 - C |\rightarrow\rangle_2 + \sqrt{1 - B^2 - C^2} |\rightarrow\rangle_3 \\ \sqrt{1 - B^2 - C^2} |\leftarrow\rangle_1 - C |\leftarrow\rangle_2 + B |\leftarrow\rangle_3 \end{cases}, \quad (27)$$

for $E = E_3^{(3)}(\mathbf{k})$. We omitted the index \mathbf{k} in eqs. (25)-(27), and defined $B(\mathbf{k})$ and $C(\mathbf{k})$ as

$$B(\mathbf{k}) \equiv \frac{t_{\perp}^2}{(\alpha'(\mathbf{k}) + \sqrt{\alpha'(\mathbf{k})^2 + 2t_{\perp}^2})\sqrt{\alpha'(\mathbf{k})^2 + 2t_{\perp}^2}}, \quad (28)$$

$$C(\mathbf{k}) \equiv \frac{t_{\perp}}{\sqrt{\alpha'(\mathbf{k})^2 + 2t_{\perp}^2}}, \quad (29)$$

respectively.

In the absence of spin-orbit coupling ($\alpha = 0$), we obtain $B(\mathbf{k}) = 1/2$ and $C(\mathbf{k}) = 1/\sqrt{2}$; then the energy bands with $E = E_1^{(3)}(\mathbf{k})$ and $E = E_3^{(3)}(\mathbf{k})$ have an even

parity with respect to the center layer, while the band $E = E_2^{(3)}(\mathbf{k})$ has the odd parity. When the spin-orbit coupling is turned on, the parity is mixed. In the limit of large spin-orbit coupling $\alpha \gg t_{\perp}$, the quasi-particle is localized on each layer, as shown in Fig. 8. The doubly degenerate wave functions are $|\rightarrow\rangle_1$ and $|\leftarrow\rangle_3$ for $E = E_1^{(3)}(\mathbf{k})$, $|\rightarrow\rangle_2$ and $|\leftarrow\rangle_2$ for $E = E_2^{(3)}(\mathbf{k})$, and $|\rightarrow\rangle_3$ and $|\leftarrow\rangle_1$ for $E = E_3^{(3)}(\mathbf{k})$.

5. Order Parameter in Band Basis

We turn to a superconducting order parameter in the band basis. For this purpose, the Hamiltonian is transformed by the unitary matrix $T(\mathbf{k})$, which diagonalizes the Hamiltonian without a pairing field ($\Delta_{ss'm}(\mathbf{k}) = 0$),

$$H = \frac{1}{2} \sum_{\mathbf{k}} \hat{C}_{\mathbf{k}}^{\dagger} \hat{H}(\mathbf{k}) \hat{C}_{\mathbf{k}} = \frac{1}{2} \sum_{\mathbf{k}} \hat{Z}_{\mathbf{k}}^{\dagger} \hat{H}'(\mathbf{k}) \hat{Z}_{\mathbf{k}}. \quad (30)$$

The basis of $\hat{Z}_{\mathbf{k}}^{\dagger}$ is chosen to be the eigenstates in eqs. (17) and (18) for bilayers. Then, we obtain the following matrix representation of the Hamiltonian;

$$\hat{H}'(\mathbf{k}) = \hat{T}^{\dagger}(\mathbf{k}) \hat{H}(\mathbf{k}) \hat{T}(\mathbf{k})$$

$$= \begin{pmatrix} E_1^{(2)} & 0 & 0 & 0 & \Delta_1 & 0 & \Delta_{13} & 0 \\ 0 & E_1^{(2)} & 0 & 0 & 0 & \Delta_2 & 0 & \Delta_{24} \\ 0 & 0 & E_2^{(2)} & 0 & \Delta_{31} & 0 & \Delta_3 & 0 \\ 0 & 0 & 0 & E_2^{(2)} & 0 & \Delta_{42} & 0 & \Delta_4 \\ \Delta_1^* & 0 & \Delta_{31}^* & 0 & -E_1^{(2)} & 0 & 0 & 0 \\ 0 & \Delta_2^* & 0 & \Delta_{42}^* & 0 & -E_1^{(2)} & 0 & 0 \\ \Delta_{13}^* & 0 & \Delta_3^* & 0 & 0 & 0 & -E_2^{(2)} & 0 \\ 0 & \Delta_{24}^* & 0 & \Delta_4^* & 0 & 0 & 0 & -E_2^{(2)} \end{pmatrix}, \quad (31)$$

where the index \mathbf{k} is omitted for simplicity.

Since we consider a small superconducting gap $|\Delta| \ll |\alpha|$, as realized in most (locally) non-centrosymmetric superconductors, the role of interband Cooper pairing is ignored. Then, the superconducting order parameter of each band is described by $\Delta_i(\mathbf{k})$ because the 2×2 matrix for intraband Cooper pairing is diagonalized in this representation. Thus, the superconductivity in bilayers is regarded as an equal pseudo-spin pairing state on the basis of eqs. (17) and (18).

The superconducting order parameter in each band is obtained as follows. There are two cases with respect to the interlayer phase difference, as discussed in §2. In case (A), the spin triplet order parameter (d-vector) has the same sign in both layers 1 and 2, while the spin singlet order parameter has opposite signs in the two layers, namely, $(\psi_1, \psi_2) = (\psi, -\psi)$ and $(d_1, d_2) = (d, d)$. In case (B), the spin singlet order parameter has the same sign in layers 1 and 2, but the d-vector has opposite signs in the two layers, namely, $(\psi_1, \psi_2) = (\psi, \psi)$ and $(d_1, d_2) = (d, -d)$.

Case (A) leads to the order parameter in the band basis for $\mathbf{k} = (0, k_y)$:

$$\Delta_1(\mathbf{k}) = -k_y \left[\frac{\alpha}{\sqrt{\alpha^2 |\mathbf{g}(\mathbf{k})|^2 + t_{\perp}^2}} \psi + d \right], \quad (32)$$

$$\Delta_2(\mathbf{k}) = \Delta_1(\mathbf{k}), \quad (33)$$

$$\Delta_3(\mathbf{k}) = -k_- \left[\frac{\alpha}{\sqrt{\alpha^2 |\mathbf{g}(\mathbf{k})|^2 + t_\perp^2}} \psi - d \right], \quad (34)$$

$$\Delta_4(\mathbf{k}) = \Delta_3(\mathbf{k}), \quad (35)$$

where $k_\pm \equiv \sin k_y \pm i \sin k_x$. On the other hand, we obtain the following results in case (B):

$$\Delta_1(\mathbf{k}) = \frac{k_-}{|\mathbf{g}(\mathbf{k})|} \left[\psi + \frac{\alpha |\mathbf{g}(\mathbf{k})|^2}{\sqrt{\alpha^2 |\mathbf{g}(\mathbf{k})|^2 + t_\perp^2}} d \right], \quad (36)$$

$$\Delta_2(\mathbf{k}) = -\Delta_1(\mathbf{k}), \quad (37)$$

$$\Delta_3(\mathbf{k}) = -\frac{k_-}{|\mathbf{g}(\mathbf{k})|} \left[\psi - \frac{\alpha |\mathbf{g}(\mathbf{k})|^2}{\sqrt{\alpha^2 |\mathbf{g}(\mathbf{k})|^2 + t_\perp^2}} d \right], \quad (38)$$

$$\Delta_4(\mathbf{k}) = -\Delta_3(\mathbf{k}). \quad (39)$$

Thus, the relative sign of $\Delta_1(\mathbf{k})$ and $\Delta_2(\mathbf{k})$ and that of $\Delta_3(\mathbf{k})$ and $\Delta_4(\mathbf{k})$ are different in cases (A) and (B) and thus also yield different spin susceptibilities, as shown in Fig. 2 and discussed in §7. We do not show the superconducting order parameter in the trilayer systems, but it is straightforward to extend our analytical calculation to trilayers.

6. Spin Susceptibility

6.1 Pauli and Van-Vleck contributions

We provide here the theoretical basis of our numerical results of spin susceptibility in §3. For this purpose, we decompose the spin susceptibility in the normal state into the Pauli and Van-Vleck parts. With the use of the linear response theory, the transverse component of uniform spin susceptibility is obtained in the normal state as

$$\begin{aligned} \chi_n^{+-} &= \lim_{q \rightarrow 0} \sum_{\eta, \nu} \sum_{\mathbf{k}} \langle \eta | S^+ | \nu \rangle \langle \nu | S^- | \eta \rangle \\ &\quad \times \frac{f(E_\eta(\mathbf{k})) - f(E_\nu(\mathbf{k} + \mathbf{q}))}{E_\nu(\mathbf{k} + \mathbf{q}) - E_\eta(\mathbf{k})}, \end{aligned} \quad (40)$$

which is decomposed into

$$\chi_n^{+-} = \chi^P + \chi^V. \quad (41)$$

The Pauli spin susceptibility χ^P arises from the intraband contributions, while the interband polarization gives rise to the Van-Vleck spin susceptibility χ^V . They can be expressed as

$$\chi^P = \sum_{E_\eta = E_\nu} \sum_{\mathbf{k}} \langle \eta | S^+ | \nu \rangle \langle \nu | S^- | \eta \rangle \delta(E_\eta(\mathbf{k})), \quad (42)$$

$$\chi^V = \sum_{E_\eta \neq E_\nu} \sum_{\mathbf{k}} \langle \eta | S^+ | \nu \rangle \langle \nu | S^- | \eta \rangle \frac{f(E_\eta(\mathbf{k})) - f(E_\nu(\mathbf{k}))}{E_\nu(\mathbf{k}) - E_\eta(\mathbf{k})}, \quad (43)$$

respectively. In multilayer systems, the Fermi surfaces are split by both spin-orbit coupling and interlayer coupling, whereby the former gives rise to the Van-Vleck susceptibility.

For the discussion of the spin susceptibility on the basis of the single-particle wave functions given in §4, it should be noted that the spin quantization axis is directed along

the ab -plane in the entire Brillouin zone. Since the spin quantization axis is perpendicular to the c -axis, the spin susceptibility along the c -axis is given by the transverse spin component that can be calculated using eq. (40).

The Van-Vleck spin susceptibility is negligibly affected by the superconducting gap when the band splitting due to the spin-orbit coupling and interlayer coupling is much larger than the superconducting gap. Thus, the Van-Vleck contribution provides a lower limit of spin susceptibility in the superconducting state. On the other hand, the Pauli spin susceptibility may be suppressed by the superconductivity and depends strongly on the symmetry of the order parameter. We will show that the Pauli spin susceptibility of multilayer superconductors is determined by the phase difference of the order parameter, which has been discussed for bilayers in §5, irrespective of the ratio of the spin singlet and the triplet order parameters. The Pauli spin susceptibility is completely suppressed in case (B), whereas it remains unaffected in case (A), as will be shown in §7.

We assumed case (A) [case (B)] in the dominant spin triplet (singlet) pairing state for the numerical calculation in §3. Thus, the spin susceptibility in the dominantly spin singlet superconducting state studied in §3 coincides with the Van-Vleck part in the normal state, and therefore $\chi_s/\chi_n = \chi^V/(\chi^P + \chi^V)$, but $\chi_s/\chi_n = 1$ in the dominantly spin triplet superconducting state. We discuss the Pauli and Van-Vleck spin susceptibilities of bi- and trilayers below.

6.2 Bilayer system

With the use of the single-particle wave functions eqs. (17) and (18) in the bilayer system, we obtain the normal state Pauli and Van-Vleck spin susceptibilities at $T = 0$ as

$$\chi^P = \sum_{\mathbf{k}} 4A(\mathbf{k})^2 (1 - A(\mathbf{k})^2) [\delta(E_1^{(2)}(\mathbf{k})) + \delta(E_2^{(2)}(\mathbf{k}))] \quad (44)$$

$$\sim \rho(0) \langle 4A(\mathbf{k})^2 (1 - A(\mathbf{k})^2) \rangle_{\text{FS}}, \quad (45)$$

and

$$\chi^V = \sum_{\mathbf{k}} 2(1 - 2A(\mathbf{k})^2)^2 \frac{\Theta(E_1^{(2)}(\mathbf{k})) - \Theta(E_2^{(2)}(\mathbf{k}))}{E_2^{(2)}(\mathbf{k}) - E_1^{(2)}(\mathbf{k})} \quad (46)$$

$$\sim \rho(0) \langle (1 - 2A(\mathbf{k})^2)^2 \rangle_{\text{FS}}, \quad (47)$$

respectively. Note that the Fermi-Dirac distribution function $f(E)$ is reduced to the step function $\Theta(E)$ at $T = 0$. The average on the Fermi surface is denoted as $\langle \cdots \rangle_{\text{FS}}$ and $\rho(0)$ is the density of state at the Fermi level.

In the absence of spin-orbit coupling, the Van-Vleck part vanishes and the Pauli part is obtained as $\chi^P = \chi_n^{+-}$ because of $A(\mathbf{k}) = 1/\sqrt{2}$. On the other hand, the Pauli part vanishes for $t_\perp = 0$ such that $\chi^V = \chi_n^{+-}$ because of $A(\mathbf{k}) = 0$.

We show the numerical results of $\chi^V/(\chi^P + \chi^V)$ obtained using eqs. (44) and (46) for various spin-orbit couplings α in Fig. 9. We see that the Van-Vleck part of the spin susceptibility in the normal state, $\chi^V/(\chi^P + \chi^V)$,

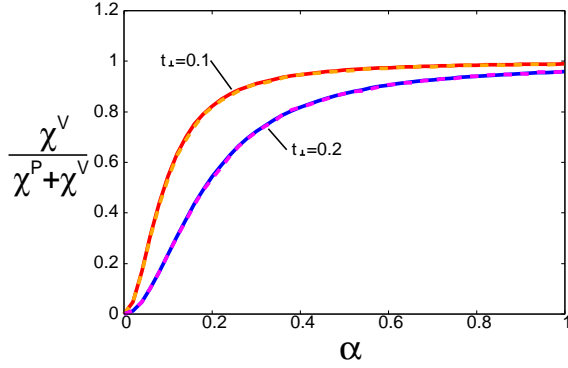


Fig. 9. (Color online) Van-Vleck part of spin susceptibility along c -axis in normal state of bilayer system, $\chi^V/(\chi^P + \chi^V)$ (solid lines). The dashed lines show the spin susceptibility in the superconducting state, χ_s/χ_n , for $\psi = 0.01$ and $d = 0$, which is shown in Fig. 2. We see that these quantities coincide with each other. The parameter is chosen as $t_\perp = 0.1$ or 0.2 .

bility, χ_s/χ_n , in the superconducting state with a dominant spin singlet order parameter. Thus, we obtain an estimate of the spin susceptibility in the superconducting state through the Van-Vleck spin susceptibility in the normal state.

6.3 Trilayer system

With the use of the single-particle wave functions eqs. (25)-(27) in the trilayers, the normal state Pauli spin susceptibility at $T = 0$ is obtained as

$$\chi^P = \sum_{\mathbf{k}} \left\{ (2B\sqrt{1-B^2-C^2} + C^2)^2 [\delta(E_1^{(3)}) + \delta(E_3^{(3)})] + (1-4C^2)^2 \delta(E_2^{(3)}) \right\} \quad (48)$$

$$\sim \frac{2\rho(0)}{3} \langle (2B\sqrt{1-B^2-C^2} + C^2)^2 \rangle_{\text{FS}} + \frac{\rho(0)}{3} \langle (1-4C^2)^2 \rangle_{\text{FS}}, \quad (49)$$

while the Van-Vleck spin susceptibility is obtained as

$$\chi^V = \sum_{\mathbf{k}} \left\{ 2C^2 (\sqrt{1-B^2-C^2} + \sqrt{1-2C^2} - B)^2 \times \left[\frac{\Theta(E_1^{(3)}) - \Theta(E_2^{(3)})}{E_2^{(3)} - E_1^{(3)}} + \frac{\Theta(E_2^{(3)}) - \Theta(E_3^{(3)})}{E_3^{(3)} - E_2^{(3)}} \right] + 2(1-2C^2)^2 \frac{\Theta(E_1^{(3)}) - \Theta(E_3^{(3)})}{E_3^{(3)} - E_1^{(3)}} \right\} \quad (50)$$

$$\sim \frac{2\rho(0)}{3} \langle 2C^2 (\sqrt{1-B^2-C^2} + \sqrt{1-2C^2} - B)^2 \rangle_{\text{FS}} + \frac{\rho(0)}{3} \langle 2(1-2C^2)^2 \rangle_{\text{FS}}, \quad (51)$$

where we omitted the index \mathbf{k} in $E_i^{(3)}(\mathbf{k})$, $B(\mathbf{k})$, and $C(\mathbf{k})$ for simplicity.

The Van-Vleck spin susceptibility vanishes in the absence of the spin-orbit coupling $\alpha = 0$, and $\chi^V \sim 2\rho(0)/3 = 2\chi_n/3$ in the limit of large spin-orbit coupling

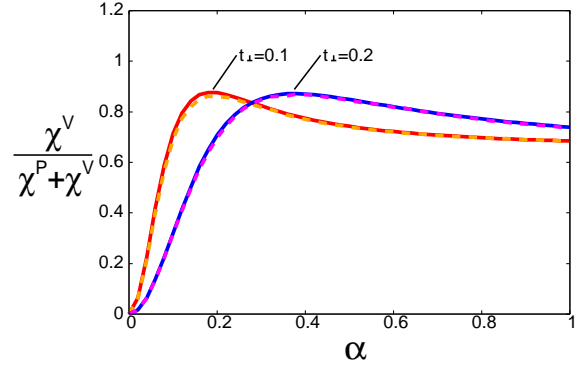


Fig. 10. (Color online) Van-Vleck part of spin susceptibility along c -axis in normal state of trilayer system, $\chi^V/(\chi^P + \chi^V)$ (solid lines). The dashed lines show the spin susceptibility in the superconducting state, χ_s/χ_n , for $\psi = 0.01$ and $d = 0$, which is shown in Fig. 3. We see that these quantities coincide with each other, as in the bilayer systems. The parameter is chosen as $t_\perp = 0.1$ or 0.2 .

$\alpha \gg t_\perp$, as expected from the discussions in §3 and §6.1. Figure 10 shows that the Van-Vleck part of the spin susceptibility in the normal state $\chi^V/(\chi^P + \chi^V)$ given by eqs. (48) and (50) coincides with the spin susceptibility in the superconducting state χ_s/χ_n , which is shown in Fig. 3. Figure 10 shows that the Pauli spin susceptibility is completely suppressed in the dominant spin singlet pairing state; therefore, the spin susceptibility of trilayers at $T = 0$ is given by the Van-Vleck part, as in the bilayer system.

7. Relation to Symmetry of Superconductivity

In this section, we examine the relation between the order parameter and spin susceptibility in our multilayer superconductors. As we discussed in §6, the Van-Vleck part of the spin susceptibility is not affected by superconductivity. On the other hand, the Pauli spin susceptibility has a clear dependence on the superconducting order parameter. Indeed, as we will show later, the Pauli spin susceptibility is determined by the phase difference of the order parameter between layers, and is essentially independent of the ratio of parity mixing, $|\psi|/|d|$.

For the bilayer system, we consider cases (A) and (B), discussed in §5, to optimize the interlayer Josephson coupling energy.

To understand the above-described aspect of the order parameter structure, it is important to view the situation in the band basis, as in eqs. (32)-(39). For $\mathbf{k} = (0, k_y)$, in the band basis, the "d-vector" of the pseudo-spin points along the y -axis in case (A) because $\Delta_1(\mathbf{k}) = \Delta_2(\mathbf{k})$ and $\Delta_3(\mathbf{k}) = \Delta_4(\mathbf{k})$. On the other hand, in case (B) the "d-vector" is oriented along the x -axis, whereby we find $\Delta_1(\mathbf{k}) = -\Delta_2(\mathbf{k})$ and $\Delta_3(\mathbf{k}) = -\Delta_4(\mathbf{k})$. Since the spin quantization axis is along the a -axis of tetragonal crystals for $\mathbf{k} = (0, k_y)$, the crystal c -axis corresponds to the y -axis with the z -axis being the spin quantization axis. Thus, the "d-vector" of a pseudo-spin is parallel to the c -axis in case (A) and perpendicular to the c -axis in case (B). This is true not only for $\mathbf{k} = (0, k_y)$ but also for all momenta in the Brillouin zone. One may mistakenly conclude that the Pauli spin susceptibility for fields along the

c -axis is suppressed (unchanged) in case (A) [case (B)] similarly to a spin triplet superconductor with a d -vector parallel (perpendicular) to the field. However, the opposite relation is actually obtained for the "d-vector" in the band basis, because the spin of each band is inversely polarized for \mathbf{k} and $-\mathbf{k}$. Therefore, taking into account the opposite sign of the spin quantization axis, it is shown that the Pauli spin susceptibility along the c -axis remains unchanged by the superconductivity in case (A), while it is completely suppressed in case (B).

We conclude here that the spin susceptibility is determined by the interlayer phase difference of the order parameters and independent of their amplitude. This surprising result has already been anticipated from Fig. 5. The spin susceptibility is nearly constant for ψ , although it shows a jump at $|\psi| = |d|$, following the discontinuity of the phase difference. Note that we assumed case (A) for $|\psi| < |d|$ and case (B) for $|\psi| > |d|$.

The above finding is confirmed by calculating the spin susceptibility while assuming case (A) or (B) regardless of the amplitude of singlet and triplet order parameters. Figure 11(a) shows the result in case (A), while Fig. 11(b) shows that in case (B). It is shown that the spin susceptibility at $T = 0$ is nearly independent of the ratio of parity mixing from $|\psi|/|d| = 0$ to $|\psi|/|d| = \infty$. Thus, the spin susceptibility remains unchanged when the dominant order parameter is a spin singlet component with a π -phase difference. On the other hand, the Pauli spin susceptibility is completely suppressed by the spin triplet order parameter with a π -phase difference between layers. In other words, the spin singlet order parameter with a π -phase difference plays the role of a spin triplet order parameter with a zero-phase difference, and *vice versa*.

We obtain the same conclusion for the trilayer systems. The spin susceptibility at $T = 0$ is determined by the phase difference and is independent of the amplitude of the order parameters. We confirmed that the spin susceptibility of trilayer superconductors is nearly constant for $|\psi|/|d|$, as in Fig. 11.

8. More than Three Layers

Finally, we show the numerical results of the spin susceptibility for systems with 4, 5, 6, and 7 layers. Superconductivity has been observed on the artificial superlattice of CeCoIn₅ with 3, 4, 5, 7, and 9 layers.⁴² We consider the dominantly spin singlet pairing state with $\psi_m = 0.01$ and ignore the spin triplet component. The subdominant component negligibly changes the spin susceptibility, as in the bi- and tri-layer systems.

In this situation, it is necessary to extend the layer dependence of the Rashba spin-orbit coupling, which is assumed to be weaker but still existent in inner layers. For illustration, we choose two distinct layer dependences of spin-orbit coupling, as we have no *ab initio* basis for our model. First, we consider a slow reduction (screening) of spin-orbit coupling, assuming a decay proportional to the inverse square of layer distance. Such a model yields $(\alpha_1, \alpha_2, \alpha_3, \alpha_4) = \alpha(1, 9/49, -9/49, -1)$ for the 4-layer system, and $(\alpha_1, \alpha_2, \alpha_3, \alpha_4, \alpha_5) = \alpha(1, 9/41, 0, -9/41, -1)$ for the 5-layer system. On the

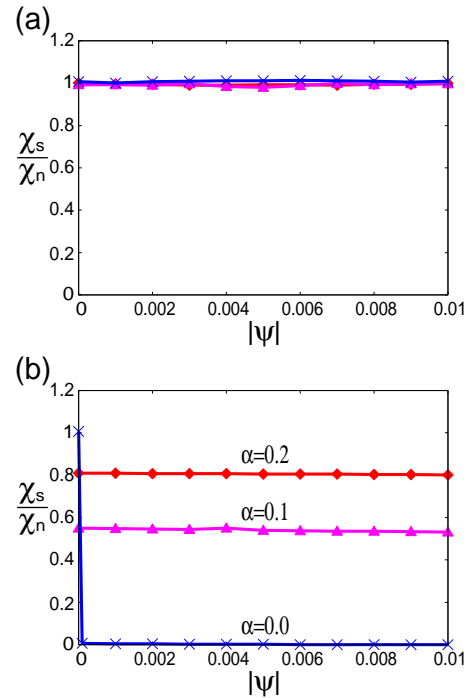


Fig. 11. (Color online) C -axis spin susceptibility in bilayer system for various $|\psi|$ values while keeping summation $|\psi| + |d| = 0.01$. The ratio $|\psi|/|d|$ changes from 0 to ∞ . We fix the phase difference of the order parameters for the two layers, irrespective of the ratio $|\psi|/|d|$, although interlayer Josephson coupling favors the zero phase difference of the dominant order parameter, as in §3. (a) Case (A) in which spin singlet order parameter has a π -phase difference between layers. (b) Case (B) in which spin singlet order parameter has a zero-phase difference. We show the results for the interlayer coupling $t_{\perp} = 0.1$ and the spin-orbit coupling $\alpha = 0$ (crosses), $\alpha = 0.1$ (triangles), and $\alpha = 0.2$ (diamonds).

ties for different multilayer systems, as shown in Fig. 12. We observe a nonmonotonic α -dependence of the spin susceptibility because, in our model, spin-orbit coupling has several crossover scales (marked by several maxima) at $\alpha_1 \sim t_{\perp}$, $\alpha_2 \sim t_{\perp}$, and so on. For large $\alpha \gg t_{\perp}$, χ_s recovers the normal state value χ_n for even numbers of layers, such as 4 and 6, whereas $\chi_s/\chi_n \rightarrow (M-1)/M$ for odd numbers of layers, because the center layer has no Rashba spin-orbit coupling.

Next, we consider an extreme situation in which Rashba spin-orbit coupling only exists for the outermost layers, i.e., $\alpha_m = 0$ except the outer layers $\alpha_1 = \alpha$ and $\alpha_M = -\alpha$. In this case, the spin susceptibility shows a single peak at approximately $\alpha \sim t_{\perp}$ (Fig. 13), as in the trilayer systems. For large spin-orbit coupling $\alpha \gg t_{\perp}$, the spin susceptibility approaches $\chi_s/\chi_n = 2/M$.

Figures 12 and 13 show nontrivial behaviors of the spin susceptibility for multilayer systems, which is affected qualitatively by the layer dependence of Rashba spin-orbit coupling. Recently, the magnetic properties of superconducting multilayer cuprates have been investigated by NMR measurements.^{53,54} In view of our discussion above, it would be interesting to perform similar NMR measurements to study the local spin polarization and to identify the effect of symmetry-induced spin-orbit coupling in multilayer superconductors.

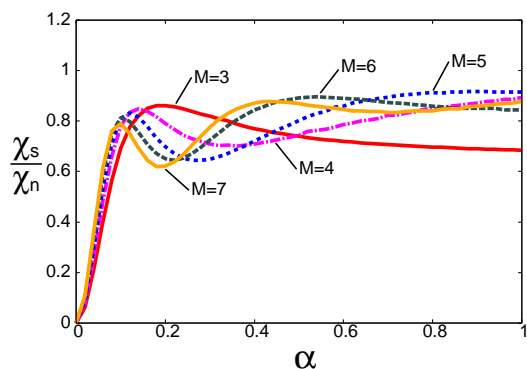


Fig. 12. (Color online) Spin susceptibilities along c -axis for $M = 3, 4, 5, 6,$ and 7 . We assume a weak screening effect of Rashba spin-orbit coupling, as explained in the text. We assume the uniform spin singlet superconducting order parameter $\psi_m = 0.01$ and the interlayer coupling $t_{\perp} = 0.1$.

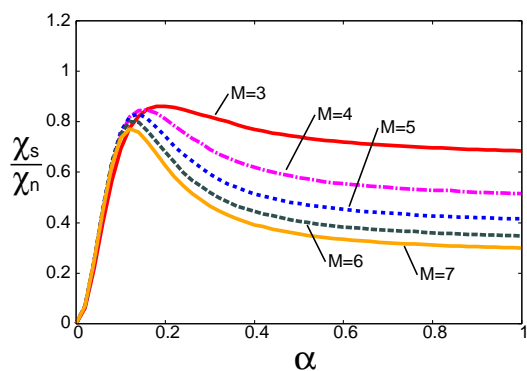


Fig. 13. (Color online) Spin susceptibility along c -axis in more than three layer systems with strong screening effect of Rashba spin-orbit coupling. Details are explained in the text. The other parameters are the same as those in Fig. 12.

9. Summary and Discussion

Motivated by the recent investigation of artificially fabricated superstructures of $\text{CeCoIn}_5/\text{YbCoIn}_5$, we have theoretically analyzed the basic properties of *locally* non-centrosymmetric superconductors in which spatially modulated Rashba spin-orbit coupling plays an important role. The single-particle wave function, superconducting gap, and spin susceptibility in the superconducting state have been determined.

Although these layered systems possess a center of inversion symmetry, they display local non-centrosymmetry that affects the spin polarizability of the superconducting phase in an interesting way. We clearly observe distinct regimes for the response of such a layered superconductor with strong or weak interlayer coupling. Although the former case exhibits a rather conventional response in the spin polarization to an external field, the latter reflects properties close to those expected for non-centrosymmetric superconductors. An intuitive understanding of the crossover between the two regimes is obtained if we decompose the spin susceptibility into the conventional Pauli and an additional Van-Vleck contributions. The latter results from a spin-orbit

coupling-induced interband contribution, which is only weakly modified by superconductivity, while the Pauli part, as an intraband contribution, depends on details of the superconducting order parameter. In the discussion of our model, we demonstrated that the response is determined by the interlayer phase structure of the order parameters, but is independent of the ratio of the magnitudes of the singlet and triplet components.

A special situation appears for dominant spin triplet pairing, which has the same phase for all layers. In this case, the spin susceptibility along the c -axis is the same as that in the normal state and is basically independent of spin-orbit coupling. On the other hand, for the dominant spin singlet pairing, the Pauli contribution to the spin susceptibility is completely suppressed at $T = 0$. Here, only the Van-Vleck susceptibility induced by layer-modulated Rashba spin-orbit coupling yields a finite contribution, depending on the interlayer coupling. The detailed orbital symmetry of order parameters, such as the s -, p -, and d -wave, affects these findings only weakly.

Our study gives the first account of the spin polarizability of superconductivity in superconductors with local non-centrosymmetry in clean artificially layered superconductors. Previous studies based on similar concepts have addressed dirty s -wave superconductors⁵⁷⁾ and random spin triplet superconductors.⁴⁰⁾ Thus, it is also interesting to review superconductors with intrinsic multilayer structures, such as some high- T_c cuprates, focusing on the role of broken local inversion symmetry. An additional feature that has been discussed recently is the effect of staggered antisymmetric spin-orbit coupling on superconductivity in some classes of centrosymmetric crystals that also belong to a similar class.⁵⁸⁾

Finally, we return to the system that initially triggered our study, the superlattice of CeCoIn_5 .⁴²⁾ In view of the fact that bulk CeCoIn_5 is known to realize spin singlet superconductivity, we believe that the dominantly spin singlet pairing state is relevant for the multilayer CeCoIn_5 in the superlattice. Unfortunately, experimental data of spin susceptibility in the superconducting state are not yet available. However, the effect of superconductivity on the spin susceptibility may be roughly estimated using the upper critical field H_{c2} , because the H_{c2} of CeCoIn_5 is determined by the paramagnetic depairing effect. From a rough estimation,

$$H_{c2} = \frac{H^P}{\sqrt{1 - \chi_s/\chi_n}}, \quad (52)$$

where H^P is the Pauli-limited upper critical field in conventional spin singlet superconductors, the large enhancement of the upper critical fields observed in the superlattice of CeCoIn_5 might be caused by spatially modulated Rashba spin-orbit coupling and may not necessary be a signature of strong-coupling effects.⁴²⁾ Moreover, we believe that the variability of the superlattices and also the possibility of the local measurements of magnetic properties by NMR measurement would give new insights into spin-orbit coupling in these artificial systems. Moreover, in this context, the fate of the magnetic quantum critical point of CeCoIn_5 is an issue that

arouses experimental and theoretical interest.

Acknowledgements

The authors are grateful to H. Shishido, T. Shibauchi, Y. Matsuda, M. Fischer, and D. F. Agterberg for fruitful discussions. D. M. thanks Y. Yamakawa for help with the numerical calculation. This work was supported by a Grant-in-Aid for Scientific Research on Innovative Areas “Heavy Electrons” (No. 21102506) from MEXT, Japan. It was also supported by a Grant-in-Aid for Young Scientists (B) (No. 20740187) from JSPS. We are also grateful for the financial support from the Swiss Nationalfonds, the NCCR MaNEP, and the Pauli Center of ETH Zurich.

- 1) E. Bauer, G. Hilscher, H. Michor, C. Paul, E. W. Scheidt, A. Griбанov, Y. Seropegin, H. Noël, M. Sigrist, and P. Rogl: Phys. Rev. Lett. **92** (2004) 027003.
- 2) To be published in *Non-centrosymmetric Superconductivity*, ed. M. Sigrist and E. Bauer (Springer).
- 3) E. Bauer, I. Bonalde, and M. Sigrist: Low. Temp. Phys. **31** (2005) 748.
- 4) E. Bauer, H. Kaldarar, A. Prokofiev, E. Royanian, A. Amato, J. Sereni, W. Brämer-Escamilla, and I. Bonalde: J. Phys. Soc. Jpn. **76** (2007) 051009.
- 5) T. Akazawa, H. Hidaka, H. Kotegawa, T. C. Kobayashi, T. Fujiwara, E. Yamamoto, Y. Haga, R. Settai, and Y. Ōnuki: J. Phys. Soc. Jpn. **73** (2004) 3129.
- 6) N. Kimura, K. Ito, K. Saitoh, Y. Umeda, H. Aoki, and T. Terashima: Phys. Rev. Lett. **95** (2005) 247004.
- 7) N. Kimura, Y. Muro, and H. Aoki: J. Phys. Soc. Jpn. **76** (2007) 051010.
- 8) I. Sugitani, Y. Okuda, H. Shishido, T. Yamada, A. Thamizhavel, E. Yamamoto, T. D. Matsuda, Y. Haga, T. Takeuchi, R. Settai, and Y. Ōnuki: J. Phys. Soc. Jpn. **75** (2006) 043703.
- 9) R. Settai, T. Takeuchi, and Y. Ōnuki: J. Phys. Soc. Jpn. **76** (2007) 051003.
- 10) M. Measson, R. Settai, and Y. Ōnuki: private communication; see also, A. Thamizhavel, H. Shishido, Y. Okuda, H. Harima, T. D. Matsuda, Y. Haga, R. Settai, and Y. Ōnuki: J. Phys. Soc. Jpn. **75** (2006) 044711.
- 11) K. Togano, P. Badica, Y. Nakamori, S. Orimo, H. Takeya, and K. Hirata: Phys. Rev. Lett. **93** (2004) 247004; P. Badica, T. Kondo, and K. Togano: J. Phys. Soc. Jpn. **74** (2005) 1014; see also, H. Q. Yuan, D. F. Agterberg, N. Hayashi, P. Badica, D. Vandervelde, K. Togano, M. Sigrist, and M. B. Salamon: Phys. Rev. Lett. **97** (2006) 017006; M. Nishiyama, Y. Inada, and G.-q. Zheng: Phys. Rev. Lett. **98** (2007) 047002.
- 12) C. Krupka, A. L. Giorgi, N. H. Krikorian, and E. G. Szklarz: J. Less-Common Met. **19** (1969) 113; G. Amano, S. Akutagawa, T. Muranaka, Y. Zenitani, and J. Akimitsu: J. Phys. Soc. Jpn. **73** (2004) 530.
- 13) T. Shibauchi, M. Nohara, H. Aruga Katori, Y. Okamoto, Z. Hiroi, and H. Takagi: J. Phys. Soc. Jpn. **76** (2007) 073708.
- 14) T. Klimczuk, Q. Xu, E. Morosan, J. D. Thompson, H. W. Zandbergen, and R. J. Cava: Phys. Rev. B **74** (2006) 220502(R); T. Klimczuk, F. Ronning, V. Sidorov, R. J. Cava, and J. D. Thompson: Phys. Rev. Lett. **99** (2007) 257004.
- 15) G. Mu, Y. Wang, L. Shan, and H.-H. Wen: Phys. Rev. B **76** (2007) 064527.
- 16) Y. L. Zuev, V. A. Kuznetsova, R. Prozorov, M. D. Vannette, M. V. Lobanov, D. K. Christen, and J. R. Thompson: Phys. Rev. B **76** (2007) 132508.
- 17) Z. Ren, J. Kato, T. Muranaka, J. Akimitsu, M. Kriener, and Y. Maeno: J. Phys. Soc. Jpn. **76** (2007) 103710.
- 18) M. Sato, Y. Takahashi, and S. Fujimoto: Phys. Rev. Lett. **103** (2009) 024041.
- 19) M. Iskin and A. I. Subasi: Phys. Rev. Lett. **107** (2011) 050402.
- 20) V. M. Edelstein: Sov. Phys. JETP **68** (1989) 1244.
- 21) V. M. Edelstein: Phys. Rev. B **72** (2005) 172501.
- 22) S. K. Yip: Phys. Rev. B **65** (2002) 144508.
- 23) S. Fujimoto: Phys. Rev. B **72** (2005) 024515.
- 24) S. Fujimoto: J. Phys. Soc. Jpn. **76** (2007) 034712.
- 25) L. N. Bulaevskii, A. A. Guseinov, and A. I. Rusinov: Sov. Phys. JETP **44** (1976) 1243.
- 26) L. P. Gor’kov and E. I. Rashba: Phys. Rev. Lett. **87** (2001) 037004.
- 27) P. A. Frigeri, D. F. Agterberg, A. Koga, and M. Sigrist: Phys. Rev. Lett. **92** (2004) 097001.
- 28) P. A. Frigeri, D. F. Agterberg, and M. Sigrist: New J. Phys. **6** (2004) 115.
- 29) K. V. Samokhin: Phys. Rev. Lett. **94** (2005) 027004.
- 30) V. P. Mineev and K. V. Samokhin: Phys. Rev. B **72** (2005) 212504.
- 31) Y. Yanase and M. Sigrist: J. Phys. Soc. Jpn. **76** (2007) 043712.
- 32) Y. Yanase and M. Sigrist: J. Phys. Soc. Jpn. **77** (2008) 124711.
- 33) Y. Yanase and M. Sigrist: J. Phys. Soc. Jpn. **76** (2007) 124709.
- 34) O. V. Dimitrova and M. V. Feigel’man: JETP Lett. **78** (2003) 637.
- 35) O. Dimitrova and M. V. Feigel’man: Phys. Rev. B **76** (2007) 014522.
- 36) K. V. Samokhin: Phys. Rev. B **70** (2004) 104521.
- 37) R. P. Kaur, D. F. Agterberg, and M. Sigrist: Phys. Rev. Lett. **94** (2005) 137002.
- 38) D. F. Agterberg and R. P. Kaur: Phys. Rev. B **75** (2007) 064511.
- 39) Y. Matsunaga, N. Hiasa, and R. Ikeda: Phys. Rev. B **78** (2008) 220508.
- 40) Y. Yanase: J. Phys. Soc. Jpn. **79** (2010) 084701.
- 41) H. Shishido, T. Shibauchi, K. Yasu, T. Kato, H. Kontani, T. Terashima, and Y. Matsuda: Science **327** (2010) 980.
- 42) Y. Mizukami, H. Shishido, T. Shibauchi, M. Shimozawa, S. Yasumoto, D. Watanabe, M. Yamashita, H. Ikeda, T. Terashima, H. Kontani, and Y. Matsuda: Nat. Phys. **7** (2011) 849.
- 43) T. Tayama, A. Harita, T. Sakakibara, Y. Haga, H. Shishido, R. Settai, and Y. Ōnuki: Phys. Rev. B **65** (2002) 180504.
- 44) H. A. Radovan, N. A. Fortune, T. P. Murphy, S. T. Hannahs, E. C. Palm, S. W. Tozer, and D. Hall: Nature **425** (2003) 51.
- 45) A. Bianchi, R. Movshovich, C. Capan, P. G. Pagliuso, and J. L. Sarrao: Phys. Rev. Lett. **91** (2003) 187004.
- 46) B.-L. Young, R. R. Urbano, N. J. Curro, J. D. Thompson, J. L. Sarrao, A. B. Vorontsov, and M. J. Graf: Phys. Rev. Lett. **98** (2007) 036402.
- 47) M. Kenzelmann, T. Strässle, C. Niedermayer, M. Sigrist, B. Padmanabhan, M. Zolliker, A. D. Bianchi, R. Movshovich, E. D. Bauer, J. L. Sarrao, and J. D. Thompson: Science **321** (2008) 1652.
- 48) J. Paglione, M. A. Tanatar, D. G. Hawthorn, E. Boaknin, R. W. Hill, F. Ronning, M. Sutherland, H. Taillefer, C. Petrovic, and P. C. Canfield: Phys. Rev. Lett. **91** (2003) 246405.
- 49) A. Bianchi, R. Movshovich, I. Vekhter, P. G. Pagliuso, and J. L. Sarrao: Phys. Rev. Lett. **91** (2003) 257001.
- 50) F. Ronning, C. Capan, A. Bianchi, R. Movshovich, A. Lacerda, M. F. Hundley, J. D. Thompson, P. G. Pagliuso, and J. L. Sarrao: Phys. Rev. B **71** (2005) 104528.
- 51) K. Izawa, K. Behnia, Y. Matsuda, H. Shishido, R. Settai, Y. Ōnuki, and J. Flouquet: Phys. Rev. Lett. **99** (2007) 147005.
- 52) J. Panarin, S. Raymond, G. Lapertot, and J. Flouquet: J. Phys. Soc. Jpn. **78** (2009) 113706.
- 53) H. Mukuda, M. Abe, Y. Araki, Y. Kitaoka, K. Tokiwa, T. Watanabe, A. Iyo, H. Kito, and Y. Tanaka: Phys. Rev. Lett. **96** (2006) 087001.
- 54) S. Shimizu, S. Tabata, H. Mukuda, Y. Kitaoka, P. M. Shirage, H. Kito, and A. Iyo: J. Phys. Soc. Jpn. **80** (2011) 043706.
- 55) M. Mori and S. Maekawa: Phys. Rev. Lett. **94** (2005) 137003.
- 56) D. Maruyama, M. Sigrist, and Y. Yanase: to be published in J. Phys.: Conf. Ser.
- 57) X. S. Wu, P. W. Adams, Y. Yang, and R. L. McCarley: Phys. Rev. Lett. **96** (2006) 127002.
- 58) M. H. Fischer, F. Loder, and M. Sigrist: Phys. Rev. B **84** (2011)